Available online at www.sciencedirect.com
ScienceDirect
International Journal of Pharmaceutics 348 (2008) 153–160
INTERNATIONAL JOURNAL OF PHARMACEUTICS
www.elsevier.com/locate/ijpharm

Pharmaceutical Nanotechnology

Surface pressure measurements in particle interaction and stability studies of poly(lactic acid) nanoparticles

S. Hirsjärvi *, L. Peltonen, J. Hirvonen

Division of Pharmaceutical Technology, Faculty of Pharmacy, P.O. Box 56, 00014 University of Helsinki, Finland

Received 4 June 2007; received in revised form 9 July 2007; accepted 10 July 2007
Available online 13 July 2007

Abstract

Stability of nanoparticle dispersion in different environments is one key issue in determining the performance and safety of the drug delivery system in question. In this study, aggregation tendency and particle–particle interactions of poly(lactic acid) nanoparticles were evaluated by their interfacial behavior upon compression. Surface pressure versus trough area (π vs. A) isotherms of the nanoparticles were registered on different subphases (pH, electrolyte concentration). The compressed particle populations were transferred to silica plates by Langmuir–Schaefer deposition and analyzed with scanning electron microscope. Aggregation of the electrostatically stabilized surfactant-free nanoparticles due to subphase alterations was clearly detected from the isotherms even though zeta potential value of the nanoparticles (−35 mV) suggested a stable system. When steric stabilization, provided by a surfactant (Poloxamer 188) in this study, was involved besides the electrostatic stabilization, the nanoparticles remained non-aggregated over a wider range of conditions. Steric stabilization together with electrostatic stabilization extended the repulsion to a longer distance.

Keywords: Poly(lactic acid); Nanoparticle; Stability; Aggregation; Surface pressure; Langmuir–Schaefer deposition

1. Introduction

Biodegradable polymeric nanoparticles have been regarded for a long time as promising devices for drug delivery (Soppimath et al., 2001; Couvreur and Vauthier, 2006). Among them, particles prepared from poly(lactic acid) (PLA) and its copolymers with poly(glycolic acid) (PLGA) fulfill the demands due to their biocompatibility and biodegradability. In addition to the successful entrapment and release of the drug, the nanoparticulate system should be stable during storage and administration. Processes such as freeze-drying as well as different liquid environments (e.g. pH, electrolyte concentration) or adsorption of proteins at the site of administration in the body might decrease the stability of nanoparticles. Aggregates thus formed could then destroy the drug delivery function of the nanoparticles or even be entrapped in capillaries in an unwanted way.

Depending on the nature of the nanoparticles, the dispersion can be stabilized either electrostatically (by the surface charge) or sterically (usually induced by surfactants), or by a combination of both (Florence and Attwood, 1998). Zeta (ζ)-potential (absolute) values higher than ±30 mV (Benita and Levy, 1993) are considered characteristic for a stable nanoparticle dispersion which is stabilized by electrostatic repulsion. According to the DLVO theory, aggregation occurs when attractive van der Waals forces between the particles become dominant (Overbeek, 1977). Loss of stability is observed as an increase in particle size deviation (detected e.g. by photon correlation spectroscopy) or by visual cloudiness, and it is usually determined by turbidity measurements; increasing turbidity indicating decreased stability (Riley et al., 1999; Trimaille et al., 2003; Vijayaraj Kumar and Jain, 2007). However, such characterizations do not provide information about the mechanism of aggregation and organization of the particles in the aggregates.

Behaviour of colloidal particles (stability, aggregation, film forming ability, etc.) at interfaces has been a topic of several studies during the last years. In these studies, e.g. metal particles such as tin oxide (Wakabayashi et al., 2006), silver (Sastry et al., 1997), gold (Mayya et al., 2003; Heriot et al., 2006), platinum

* Corresponding author. Tel.: +358 9 191 59306; fax: +358 9 191 59144.
E-mail address: samuli.hirsjarvi@helsinki.fi (S. Hirsjärvi).

0378-5173/$ – see front matter © 2007 Elsevier B.V. All rights reserved.
doi:10.1016/j.ijpharm.2007.07.008

(Sastry et al., 1998) and magnetite (Nakaya et al., 1996; Lefebure et al., 1998); glass (Hórvölgyi et al., 1996) and silica (Zhang et al., 1991; Máté et al., 1998) particles as well as polystyrene particles (Aveyard et al., 2000; Ghezzi et al., 2001; Mu and Seow, 2006; Reynaert et al., 2006) were used. Typical interfaces in these studies are water–air and water–oil (e.g. octane). Surface pressure induced by particle compression at an interface is traditionally studied by the Wilhelmy balance technique. For example, surface pressure versus surface area (π vs. A) isotherm for polystyrene particles was determined already in the 1960s (Schuller, 1967). Particles at a surface can be deposited on solid substrates by the Langmuir–Blodgett (LB) (Nakaya et al., 1996; Mayya et al., 2003; Oh et al., 2006) and Langmuir–Schaefer (LS) (Brown et al., 2001; Brust et al., 2001; Heriot et al., 2006) techniques. In the former technique, the substrate is immersed in water by vertical strokes, whereas in the latter the surface is touched by a horizontal substrate. The deposition allows further investigation of the particulate population, e.g. by electron microscope.

Although surface pressure determinations are a widely used tool in the characterization of systems prepared from inorganic particles, its application in the studying of organic nanoparticles (except polystyrene) has been less frequent (Wolert et al., 2001; Minkov et al., 2005; Oh et al., 2006). However, application of surface pressure measurements could also be expanded to the characterization pattern of biodegradable nanoparticles intended in pharmaceutical use.

Therefore, in this study, stability of poly(lactic acid) nanoparticles was characterized by surface pressure measurements. Effect of different environments (changes in pH and electrolyte concentration) and types of the nanoparticles (prepared with or without a surfactant) were determined on the particle–particle interactions and aggregation behaviour.

2. Materials and methods

2.1. Materials

PURASORB® PDL 02A poly(D,L-lactic acid) (a donation from PURAC Biomaterials, Gorinchem, The Netherlands) (IV 0.20 dl/g) formed the nanoparticulate matrix. Other excipients used in the nanoparticle preparation and characterization were acetone and sodium chloride (subphase electrolyte) (Riedel-de Haën, Seelze, Germany), Poloxamer 188 (Lutrol® F 68, BASF, Ludwigshafen, Germany), hydrochloric acid and sodium hydroxide (subphase pH alteration) (Shannon Co., Clare, Ireland), isopropanol (Sigma–Aldrich, Steinheim, Germany) and ultrapurified water (Millipore, Molsheim, France). 11 μm paper filters (Whatman, Brentford, UK) and 0.2 μm Isopore™ membrane filters (Millipore, Molsheim, France) were used for the purification of the nanoparticle dispersions.

2.2. Nanoparticle preparation

PLA nanoparticles were prepared by the nanoprecipitation method (Fessi et al., 1989). 25 mg of PLA was dissolved in 2 ml of acetone. The polymeric solution was added with a syringe and a gauge directly into 4 ml of the outer phase (water or water with the surfactant, Poloxamer 188) under mild stirring. The organic solvent was evaporated for 40 min under reduced pressure; the nanoparticle dispersion was diluted with isopropanol and filtered (paper filter) to remove possible undesired aggregates formed during the nanoprecipitation. In the case of the nanoparticles prepared with the surfactant, the dispersion was purified by filtration through membrane filter to remove the excess surfactant. The nanoparticles remaining on the membrane surface were re-diluted with isopropanol.

2.3. Nanoparticle characterization

ζ-Potential and size distribution of the nanoparticles were determined with Malvern Zetasizer 3000HS (Malvern, Worcestershire, UK) equipped with MPT-1 titrator. Electrophoretic mobilities were converted to ζ-potentials using Smoluchowski's equation. Particle sizing was based on photon correlation spectroscopy; the results were analyzed by CONTIN algorithm and the sizes presented based on the intensity distributions.

π vs. A isotherms were recorded by Wilhelmy plate technique using a KSV minitrough (KSV Instruments, Helsinki, Finland). Before spreading the nanoparticle dispersion, the barriers were compressed to the narrowest position and the subphase surface was removed by suction of a small amount of the subphase. After cleaning, the barriers were expanded and 40–75 μl of the particle dispersion was spread dropwise on the surface with a Hamilton microsyringe. The surface was compressed at a speed of 10 mm/min. Particle populations were deposited on silanized silicon plates by touching the surface with a horizontal plate (LS deposition). The plates were washed first with hydrogen fluoride (50%) – ethanol solution and then with Piranja solution prior to the treatment with trichlorooctadecylsilane (3% (v/v)) in toluene.

Appearance of the nanoparticle populations was visualized by scanning electron microscopy (SEM). Nanoparticulate samples, on the silicon plates, were sputtered for 20 s with platinum (Agar Sputter Coater, Agar Scientific Ltd., Essex, UK) and analyzed with a SEM (DSM 962, Zeiss, Jena, Germany).

3. Results and discussion

3.1. Size and ζ-potential

The PLA nanoparticles were prepared with or without the surfactant (Poloxamer 188) in the outer phase. Mean sizes and polydispersities for the surfactant-free nanoparticles were 243 nm and 0.1, and for the surfactant-containing nanoparticles 289 nm and 0.04, respectively. Although the nanoprecipitation process does not require the use of surfactant (Fessi et al., 1989), its use led, in this study, to slightly narrower size distribution and larger particle size. Surfactant adsorption on the nanoparticle surface might be one reason for the larger size of the nanoparticles.

ζ-Potential measurements were performed to evaluate the magnitude of the electrostatic stabilization at different conditions and to provide background information for the surface

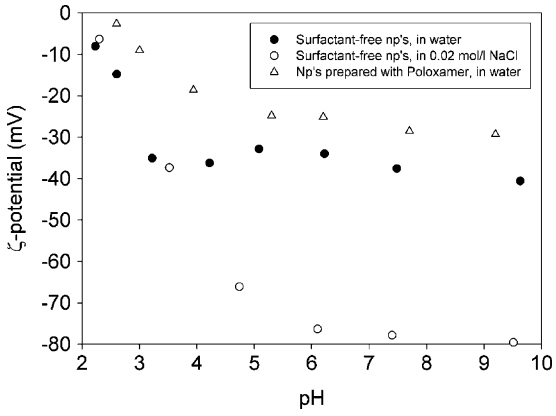

Fig. 1. ζ-Potential values of the PLA nanoparticles (np's) as a function of pH.

pressure determinations. ζ-Potential of the nanoparticles as a function of pH are presented in Fig. 1. As the pH was decreased, the magnitude of ζ-potential values decreased due to protonation of the carboxylic acid chains of the PLA particle surface at low pH values. As surfactants are not a prerequisite for a successful nanoparticle preparation process, the PLA nanoparticles were stabilized by electrostatic repulsion because of their surface charge. The essential role of surfactants in the nanoprecipitation process is assumed to be the stabilization of the liquid droplets containing the polymer before the polymer precipitation is complete (Quintanar-Guerrero et al., 1998). However, even after the precipitation, location of the surfactant molecules at the nanoparticle surface was revealed by lower ζ-potential (absolute) values, at the entire studied pH range, compared to the Poloxamer-free nanoparticles (Fig. 1). According to our previous study (also seen in Fig. 1, PLA nanoparticles in 0.02 mol/l NaCl), at neutral pH the PLA nanoparticles reached their maximum ζ-potential (absolute) value at low electrolyte concentrations (Hirsjärvi et al., 2006), as the electric double layer around the particles extended to a larger distance (Overbeek, 1977). In the case of the surfactant-free nanoparticles, when the pH was decreased to around 4 by HCl addition, the dissociated H^+ and Cl^- ions acted also as electrolytes, which surpassed the surface charge-decreasing effect of the pH decrease. This effect was masked if Poloxamer 188 was present on the nanoparticle surfaces.

3.2. π vs. A isotherms

π vs. *A* isotherms of the PLA nanoparticles on different subphases were registered to evaluate aggregation behaviour and particle–particle interactions of the nanoparticles. Isopropanol was found to be a suitable spreading dispersant: the particles could be re-dispersed from isopropanol to water without changes in either ζ-potential or size (data not shown); isopropanol also inhibited diffusion of the particles into the subphase during the spreading. The nanoparticles could be spread on all the tested subphases, although in some studies, spreading of polystyrene (Aveyard et al., 2000) and silica (Zhang et al., 1991) particles was reported to be impossible on pure water. Volumes of the particle dispersions spread on the subphases were adjusted to give an initial surface pressure value of approximately 2 mN/m. With this procedure, the isotherms could be compared better. Nanoparticulate concentrations of the spreading dispersions were not determined due to the existing polydispersity of the particles and inevitable polymer loss during nanoparticle preparation (filtration).

Generally, as the particles were compressed, the pressure was increased due to the repulsive forces between the particles. The nanoparticles on each subphase were compressed for a second time after expansion of the barriers to the initial position. The second run isotherms were, in all of the cases, superimposed with the first ones (data not shown), which indicates that the compression did not induce irreversible aggregation, particle organization or escape in the subphase.

π vs. *A* isotherms of the surfactant-free PLA nanoparticles on different pH subphases are presented in Fig. 2. Among the tested pH values, the isotherms from pH 8.0 and 5.3 were superimposed with the pure water isotherm (pH 6.5), while the isotherms at pH 4.0, 2.6 and 1.7 were comparable. No clear plateau regions in the end of compression, indicative for a collapse (e.g. considerable escape of the particles into the subphase or formation of multilayered structures) of the particulate population on the subphase, were observed from the isotherms (Fig. 2). The particles could resist the compression until the end of the cycle due to their surface charge. Only on subphases with pH 4.0 or below, slightly end-curved isotherms (at high pressure) could be observed. Electrostatic repulsion between the particles had decreased due to the less charged carboxylic acids on the PLA nanoparticle surface, and the particles could get in close contact giving rise to the attractive van der Waals forces dominant at short distances (Overbeek, 1977). In addition to the curved ends, these isotherms exhibited increase in the surface pressure at larger surface area and higher surface pressure in the end of the compression, compared to the isotherms at higher pH values. It seems obvious that the particle aggregates thus formed at low pH values resisted (mechanically) the compression more than the nanoparticulate population consisting of the more charged individual particles (pH above 4.0), which could be rearranged in a more flexible way.

PLA nanoparticles prepared with the surfactant, Poloxamer 188, were also compressed on subphases with different pH val-

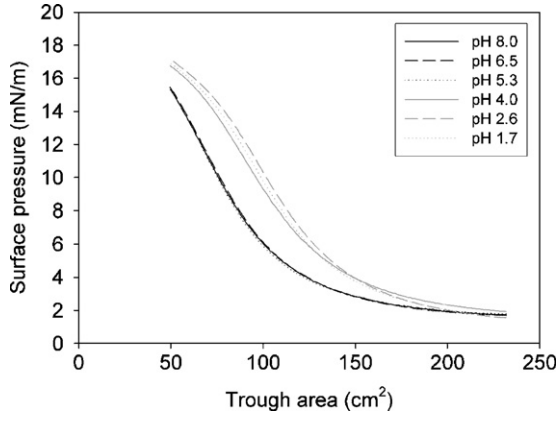

Fig. 2. π vs. *A* isotherms of the surfactant-free PLA nanoparticles on subphases at different pH values.

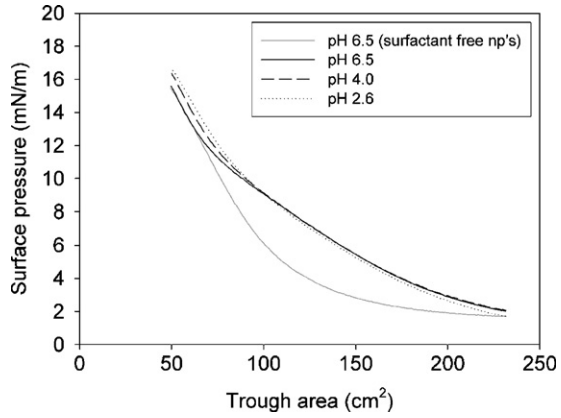

Fig. 3. π vs. A isotherms of the PLA nanoparticles (np's) prepared with Poloxamer 188 on subphases at different pH values (isotherm of the surfactant-free PLA nanoparticles is plotted in the graph for comparison purposes).

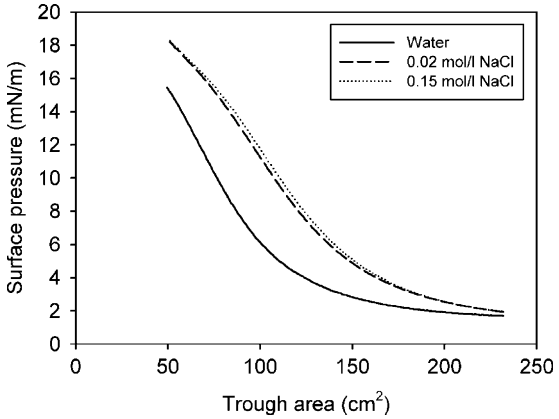

Fig. 4. π vs. A isotherms of the surfactant-free PLA nanoparticles on subphases with different amounts of the electrolyte (NaCl) added.

ues (Fig. 3). The pH values were selected based on the findings from the previous isotherms (Fig. 2: differing isotherms at pH 4.0 and below). Compared to the surfactant-free nanoparticles, isotherms from these particles exhibited more constant and linear increase of the surface pressure, which started already at larger surface area. Obviously, this indicates that the surfactant molecules, located on the nanoparticle surface, created a steric barrier that resisted the compression even at long distances. Generally, the effect of steric stabilization is short-ranged (Florence and Attwood, 1998), but probably the cumulative effect of surface charge and the surfactant resulted in increased repulsion. Interestingly, end parts of the isotherms (surfactant-free and Poloxamer 188 nanoparticles), from ~12 to 16 mN/m, were identical. An explanation could be that the surfactant-free particles, at the low compression, could move more freely on the subphase, while the steric barrier created by the Poloxamer 188 molecules restricted the movement of these particles. In the end of the compression, when the area available for the particles had decreased significantly and the particles were closer to each other, repulsion due to the surface charge became dominant in both the cases. When pH was decreased, shape of the isotherms did not change, which promotes the role of the surfactant as a shield against aggregation. Only the final surface pressure values were slightly higher, which might originate from the mechanical barrier against the compression (possible aggregates). Additionally, to reach the initial desired surface pressure after spreading, only two thirds of the volume of the surfactant-free nanoparticles was needed (40 μl vs. 60 μl). Based on these findings, both the surface charge and the surfactant seemed to have a role in the nanoparticle stabilization as also reported earlier (Trimaille et al., 2003). According to the Fig. 3, effect of the surfactant was detected at long distances, while the surface charge was dominant when the nanoparticles were at close contact.

To evaluate the effect of increased surface charge on the compression behaviour, the surfactant-free PLA nanoparticles were compressed on subphases with increased electrolyte concentration (Fig. 4). ζ-Potentials of the nanoparticles were about −75 and −45 mV in 0.02 and 0.15 mol/l NaCl, respectively. In water, the value was about −35 mV (Fig. 1). At some point, when the electrolyte concentration is increased, PLA nanoparticles are known to start to aggregate (Trimaille et al., 2003; Hirsjärvi et al., 2006), but at low concentrations the dispersion should be stable. Similarly to the isotherms from the subphases with low pH values (Fig. 2), resistance towards compression (earlier rise in the isotherm) could be detected as the electrolyte (NaCl) was added. At the end of the compression, the isotherms reached the highest surface pressure value (18 mN/m) among the tested nanoparticles and different subphases. The resistance obviously originated from the high surface charge, although in the case of 0.15 mol/l NaCl some aggregation might have occurred already. If these isotherms and the isotherms in Fig. 3 are compared, one can assume that the resistant effect of the surfactant is more long-ranged (early rise in the isotherm and slightly higher surface pressures halfway of the compression), but it allows closer packing of the particles (not an equally high pressure in the end of the compression).

Next, the nanoparticles prepared with Poloxamer 188 were compressed on the two subphases with increased electrolyte concentration (Fig. 5). These isotherms did not differ significantly from those of Fig. 3: the surfactant concealed the effects of possible increase in surface charge. In these isotherms, the

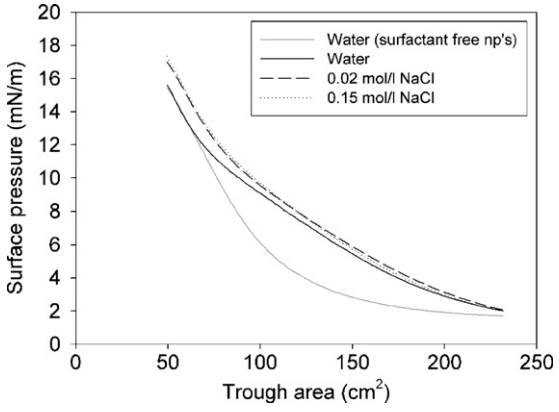

Fig. 5. π vs. A isotherms of the PLA nanoparticles (np's) prepared with Poloxamer 188 on subphases with different amounts of the electrolyte (NaCl) added (isotherm of the surfactant-free PLA nanoparticles is plotted in the graph for comparison purposes).

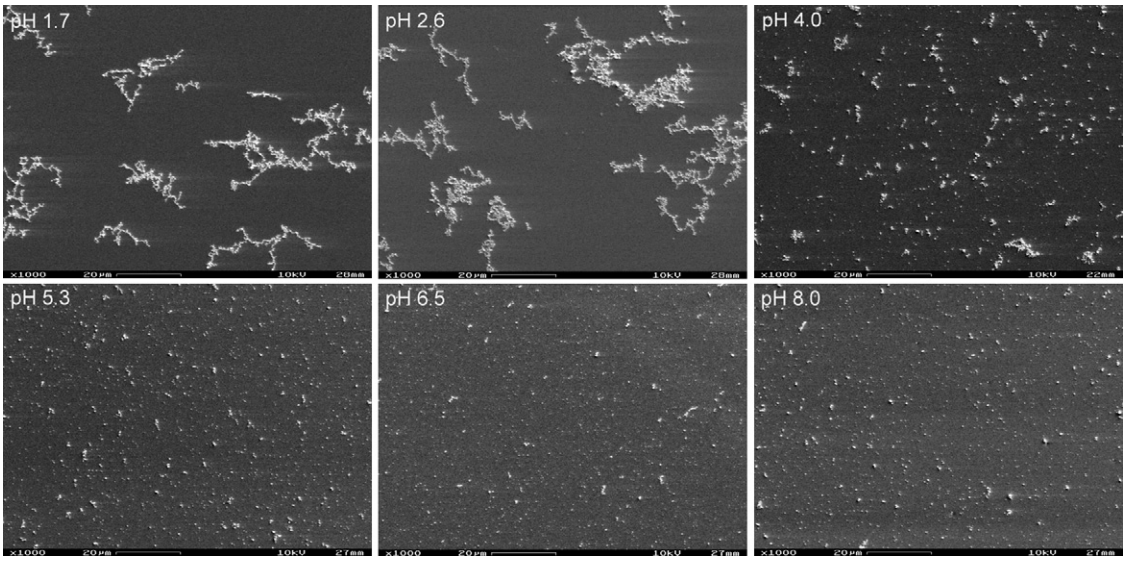

Fig. 6. SEM images of the surfactant-free PLA nanoparticles deposited from subphases at different pH values.

higher final pressures, compared to the isotherm on water, might be a consequence from the increased surface charge as in the case of surfactant-free PLA nanoparticles on the NaCl-modified subphases (Fig. 4).

3.3. Langmuir–Schaefer deposition and SEM analyses

In order to clarify the interpretations made from the π vs. A isotherms, the PLA nanoparticle populations on the subphases were deposited by the LS technique to silicon plates followed by SEM analysis. The plates were silanized by trichlorooctadecylsilane to ensure their hydrophobicity. Positively charged silicon plates, functionalized by [3-(trimethoxysilyl)propyl]octadecyldimethylammoniumchloride were also tested, but according to the SEM observations, the nanoparticles seemed to adsorb better on the non-charged, hydrophobic plates. Particle deposition was tried also using the LB technique. The particles were, however, better deposited by the LS technique as also revealed by other authors (Heriot et al., 2006). Using the LB technique, the SEM imaging revealed certain "flowing stripes" of these PLA nanoparticles on silicon plates, probably due to the vertical lifting of the plate. The depositions by the LS technique were performed at two different surface pressures: 7 mN/m (constant-rise region of the isotherms) and the most compressed state (end of the compression). No significant differences in the structures of the nanoparticle populations deposited at the different surface pressures were observed. The populations deposited at higher surface pressures were, however, denser and easier to discern. The presented SEM images are therefore from the most compressed state. As already observed from the repeatable π vs. A isotherms, these PLA nanoparticles seemed to form aggregates and clusters during the compression rather than to escape to the subphase (i.e. affinity to the interface), which has also been observed by polystyrene particles (Aveyard et al., 2000).

SEM images of the surfactant-free nanoparticles at different pH values are presented in Fig. 6. Images from pH 8.0, 6.5 and 5.3 consisted mostly of individual nanoparticles (seen as white small dots). At pH 4.0, some clusters were already present, whereas at pH 2.6 and 1.7 percolated nanoparticle networks could be seen with no individual particles at the background. These percolated particle networks are typical for a system, in which the aggregation occurs spontaneously because of the particle diffusion and collisions. The aggregation process is referred to as diffusion-limited cluster aggregation (DLCA) (Robinson and Earnshaw, 1992). Overall, the observations at different pH values are in agreement with the corresponding π vs. A isotherms: aggregation was evident at pH 4.0 (ζ-potential still being around -35 mV, Fig. 1) and below.

SEM images of the nanoparticles prepared with Poloxamer 188, deposited at different pH values, are presented in Fig. 7. At pH 6.5 and 4.0, the nanoparticles were smoothly spread on the surface and no aggregates could be detected. When the pH was decreased to 2.6, particle aggregates were present, but as a form of small clusters rather than as percolated networks. In this case, the aggregation process was reaction-limited (RLCA): compared to the DLCA regime, the probability of particle aggregation was lower (Robinson and Earnshaw, 1992; Reynaert et al., 2006). The surfactant molecules probably prevented the particle clusters from freely diffusing and forming network-like structures. Obviously these clusters diffused and were organized similarly to the individual PLA nanoparticles during the compression, because the isotherms at pH 4.0 and 2.6 were parallel to the pH 6.5 isotherm (Fig. 3). Thus, the behaviour of these nanoparticles could not be concluded solely from the isotherms. Compared to the surfactant-free PLA nanoparticles (Fig. 6), aggregation was not observed at pH 4.0: the appearance of the nanoparticle populations in Fig. 7, at pH values of 6.5 and 4.0, was smoother. These findings promote the role of the surfactant in the stabilization of nanoparticle dispersion in addition to the electrostatic stabilization.

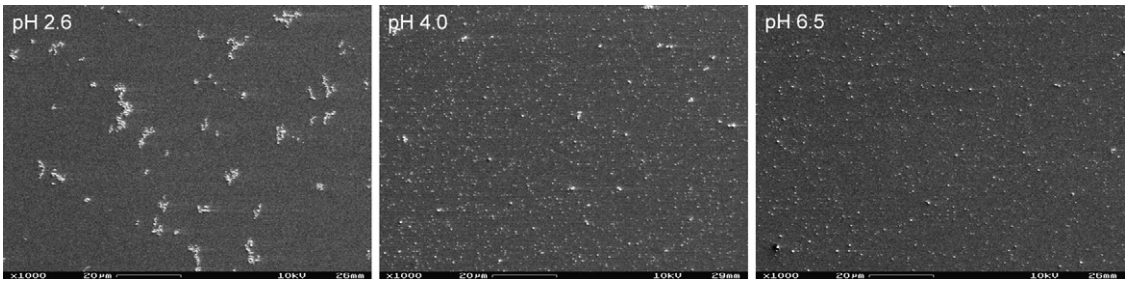

Fig. 7. SEM images of the PLA nanoparticles prepared with Poloxamer 188 deposited from subphases at different pH values.

Effect of the electrolyte addition in the subphase on both types of the PLA nanoparticles is presented in Fig. 8. In the case of surfactant-free PLA nanoparticles (above), some small clusters are visible when 0.02 mol/l NaCl was added to the subphase. This finding was interesting as the nanoparticle population was supposed to be the most stable at this electrolyte concentration because of the high surface charge (Fig. 1). Obviously that is the case in bulk, but at the compressed state the high surface charge seemed to be the cause for the cluster formation. One possible reason is high mechanical tension between the particles due to the charge and the compression leading to cluster-forming collisions. At higher electrolyte concentration (0.15 mol/l), aggregates were formed as the electrolyte screened the interparticle repulsion (Aveyard et al., 2000). This time the charge probably inhibited free diffusion and formation of the percolated networks, and the aggregates acted as the small RLCA clusters. The Poloxamer 188 PLA nanoparticles (below) were smoothly spread on 0.02 mol/l NaCl, whereas on 0.15 mol/l NaCl some minor clusters were detectable. Again, the surfactant-containing particles avoided aggregation whereas the surfactant-free PLA particles were already clustered.

According to the DLCA/RLCA classification, the RLCA clusters are more compact (Robinson and Earnshaw, 1992). In π vs. A isotherms this is observed as better compressibility of smaller clusters (Lefebure et al., 1998). Overall, if the nanoparticles were aggregated as percolated networks according to the DLCA regime (Fig. 6), it could be observed from the π vs. A isotherms as resistance against compression (Fig. 2). On the other hand, if RLCA clusters were formed (Figs. 7 and 8), the process could not be clearly seen from the corresponding π vs. A isotherms (Figs. 3–5). Therefore, it is obvious that the π vs. A isotherms described the behaviour of larger units rather than of individual nanoparticles. Thus, according to these surface pressure measurements, nanoparticles acted similarly to their non-networked aggregates upon compression.

Finally, it should be noted that the compression of the PLA nanoparticles on liquid–air interfaces does not directly describe the behaviour of the nanoparticles dispersed in the same medium. Reasonable size distributions and polydispersities can be obtained when PLA nanoparticles are freshly dispersed even in low pH media. In general, the same forces are valid for the particle interactions at the interface as well as in the bulk. However, the electrostatic repulsion between the

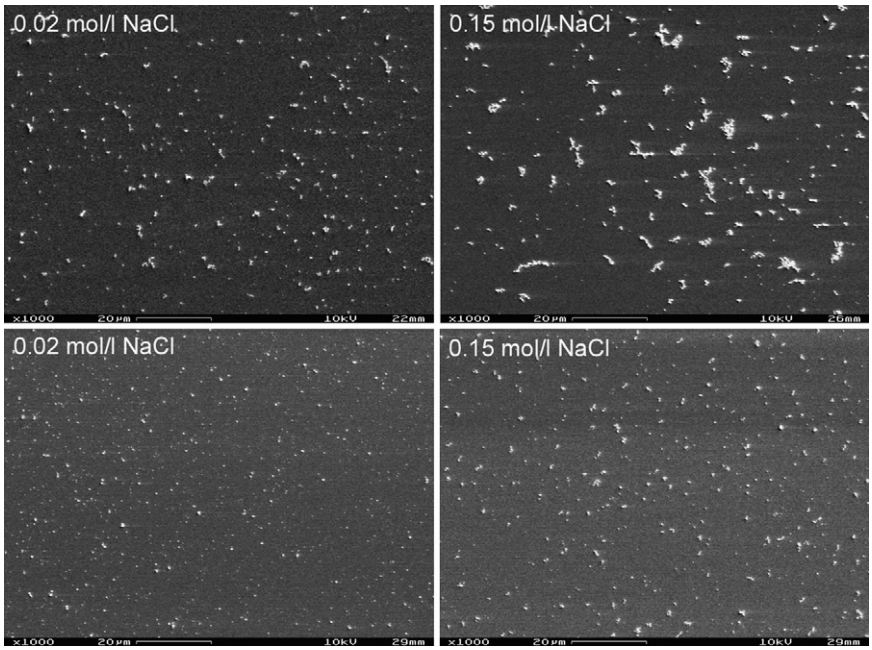

Fig. 8. SEM images of the surfactant-free PLA nanoparticles (above) and the surfactant-containing (Poloxamer 188) PLA nanoparticles (below) deposited from subphases with different amounts of added electrolyte (NaCl).

charged particles at water—low dielectric constant medium (air, oil) interface has been reported to be increased compared to the bulk (Pieranski, 1980). A particle at the interface has an asymmetric distribution of counterions, which cause a dipole moment normal to the water surface. Repulsion occurs through the low dielectric constant phase, whereas repulsion in water is screened by free ions. On the other hand, despite the possible increased repulsion, different clustered particle structures (mesostructures) are known to be formed spontaneously at the water–air interface (Ghezzi et al., 2001). When the nanoparticles are injected in the interface, interfacial turbulences (Marangoni effect) are reported to arise because of spreading of the dispersing liquid (in this study isopropanol) (Santiago-Rosanne et al., 1997). This might create forces strong enough to induce particle contacts and aggregation, which might have been the reason for cluster/aggregate formation in some cases. In addition to the van der Waals attractive forces, capillary forces are assumed to be responsible for a longer-range attraction between the particles at the interface (Pieranski, 1980; Ghezzi et al., 2001).

The ζ-potential, π vs. A isotherm and LS deposition results of the PLA nanoparticles and the subsequent conclusions presented in this study are obviously not directly applicable to all related nanoparticles. Independent evaluation of different systems provides information to compare nanoparticle properties in different environments. Combining this information might enable the creation of a general model to be utilized in the stability/aggregation evaluation of pharmaceutical nanoparticles.

4. Conclusions

π vs. A isotherms and corresponding SEM images provide information about aggregation tendency and aggregation behaviour of the PLA nanoparticles. Combined results of the π vs. A isotherms and SEM analyses suggested that the particle aggregation of the surfactant-free PLA nanoparticles during compression started already at a higher pH than what would have been expected based on the ζ-potential versus pH graphs in Fig. 1, and the aggregation could be clearly observed from the π vs. A isotherms. The nanoparticle aggregation occurred by diffusion and resulted in percolated particle networks, if the surfactant was not present. With surfactant, or if the surface charge was high enough, formation of networks was prevented and the aggregates remained as clusters. The π vs. A isotherms indicated that the steric stabilization together with the electrostatic stabilization created a repulsion that extended to longer distances, while just the electrostatic stabilization was dominant at shorter distances, at the most compressed state. Presence of the surfactant, Poloxamer 188, enhanced the stability of the systems and together with the electrostatic stabilization provided the best stability for the PLA nanoparticle dispersions against the changes in outer environment. The findings of this study promote the use of surface pressure determinations, combined with particle deposition and SEM analysis, in the stability and aggregation evaluation of pharmaceutical nanoparticles.

Acknowledgements

Research Foundation of the University of Helsinki is acknowledged for the funding of the study. Ms. Niina Suni is acknowledged for silanizing the silicon plates. Electron Microscopy Unit in the Institute of Biotechnology (University of Helsinki) is acknowledged for providing laboratory facilities and analytical equipment.

References

Aveyard, R., Clint, J.H., Nees, D., Paunov, V.N., 2000. Compression and structure of monolayers of charged latex particles at air/water and octane/water interfaces. Langmuir 16, 1969–1979.

Benita, S., Levy, M.Y., 1993. Submicron emulsions as colloidal drug carriers for intravenous administration: comprehensive physicochemical characterization. J. Pharm. Sci. 82, 1069–1079.

Brown, J.J., Porter, J.A., Daghlian, C.P., Gibson, U.J., 2001. Ordered arrays of amphiphilic gold nanoparticles in Langmuir monolayers. Langmuir 17, 7966–7969.

Brust, M., Stuhr-Hansen, N., Nørgaard, K., Christensen, J.B., Nielsen, L.K., Bjørnholm, T., 2001. Langmuir–Blodgett films of alkane chalcogenide (S,Se, Te) stabilized gold nanoparticles. Nano Lett. 1, 189–191.

Couvreur, P., Vauthier, C., 2006. Nanotechnology: intelligent design to treat complex disease. Pharm. Res. 23, 1417–1450.

Fessi, H., Puisieux, F., Devissaguet, J.P., Ammoury, N., Benita, S., 1989. Nanocapsule formation by interfacial polymer deposition following solvent displacement. Int. J. Pharm. 55, R1–R4.

Florence, A.T., Attwood, D., 1998. Physicochemical principles of pharmacy, third ed. Palgrave, Houndmills.

Ghezzi, F., Earnshaw, J.C., Finnis, M., McCluney, M., 2001. Pattern formation in colloidal monolayers at the air–water interface. J. Colloid Interface Sci. 238, 433–446.

Heriot, S.Y., Zhang, H.-L., Evans, S.D., Richardson, T.H., 2006. Multilayers of 4-methylbenzenethiol functionalized gold nanoparticles fabricated by Langmuir–Blodgett and Langmuir–Schaefer deposition. Colloids Surf. A 278, 98–105.

Hirsjärvi, S., Peltonen, L., Hirvonen, J., 2006. Layer-by-layer polyelectrolyte coating of low molecular weight poly(lactic acid) nanoparticles. Colloid Surf. B 49, 92–98.

Hórvölgyi, Z., Nemeth, S., Fendler, J.H., 1996. Monoparticulate layers of silanized glass spheres at the water–air interface: particle–particle and particle–subphase interactions. Langmuir 12, 997–1004.

Lefebure, S., Menager, C., Cabuil, V., Assenheimer, M., Gallet, F., Flament, C., 1998. Langmuir monolayers of monodispersed magnetic nanoparticles coated with a surfactant. J. Phys. Chem. B 102, 2733–2738.

Máté, M., Fendler, J.H., Ramsden, J.J., Szalma, J., Hórvölgyi, Z., 1998. Eliminating surface pressure gradient effects in contact angle determination of nano- and microparticles using a film balance. Langmuir 14, 6501–6504.

Mayya, K.M., Gole, A., Jain, N., Phadtare, S., Langevin, D., Sastry, M., 2003. Time-dependent complexation of cysteine-capped gold nanoparticles with octadecylamine Langmuir monolayers at the air–water interface. Langmuir 19, 9147–9154.

Minkov, I., Ivanova, T., Panaiotov, I., Proust, J., Saulnier, P., 2005. Reorganization of lipid nanocapsules at air–water interface. I. Kinetics of surface film formation. Colloid Surf. B 45, 14–23.

Mu, L., Seow, P.H., 2006. Application of TPGS in polymeric nanoparticulate drug delivery system. Colloids Surf. B 47, 90–97.

Nakaya, T., Li, Y.-J., Shibata, K., 1996. Preparation of ultrafine particle multilayers using the Langmuir–Blodgett technique. J. Mater. Chem. 6, 691–697.

Oh, S.W., Suh, J.H., Kang, Y.S., 2006. Preparation and characterization of ultra thin LB films using pyrazoline organic nanoparticles. Colloid Surf. A 284/285, 359–363.

Overbeek, J.T.G., 1977. Recent developments in the understanding of colloid stability. J. Colloid Interface Sci. 58, 408–422.

Pieranski, P., 1980. Two-dimensional interfacial colloidal crystals. Phys. Rev. Lett. 45, 569–572.

Quintanar-Guerrero, D., Allémann, E., Fessi, H., Doelker, E., 1998. Preparation techniques and mechanisms of formation of biodegradable nanoparticles from preformed polymers. Drug Dev. Ind. Pharm. 24, 1113–1128.

Reynaert, S., Moldenaers, P., Vermant, J., 2006. Control over colloidal aggregation in monolayers of latex particles at the oil–water interface. Langmuir 22, 4936–4945.

Riley, T., Govender, T., Stolnik, S., Xiong, C.D., Garnett, M.C., Illum, L., Davis, S.S., 1999. Colloidal stability and drug incorporation aspects of micellar-like PLA-PEG nanoparticles. Colloids Surf. B 16, 147–159.

Robinson, D.J., Earnshaw, J.C., 1992. Experimental study of colloidal aggregation in two dimensions. I. Structural aspects. Phys. Rev. A 46, 2045.

Santiago-Rosanne, M., Vignes-Adler, M., Velarde, M.G., 1997. Dissolution of a drop on a liquid surface leading to surface waves and interfacial turbulence. J. Colloid Interf. Sci. 191, 65–80.

Sastry, M., Mayya, K.S., Patil, V., Paranjape, D.V., Hegde, S.G., 1997. Langmuir–Blodgett films of carboxylic acid derivatized silver colloidal particles: role of subphase pH on degree of cluster incorporation. J. Phys. Chem. B 101, 4954–4958.

Sastry, M., Patil, V., Mayya, K.S., Paranjape, D.V., Singh, P., Sainkar, S.R., 1998. Organization of polymer-capped platinum colloidal particles at the air–water interface. Thin Solid Films 324, 239–244.

Schuller, H., 1967. Modellversuche zur spreitung von kolloid-partikeln. Kolloid Z. Z. Polym. 216/217, 380–383.

Soppimath, K.S., Aminabhavi, T.M., Kulkarni, A.R., Rudzinski, W.E., 2001. Biodegradable polymeric nanoparticles as drug delivery devices. J. Control. Release 70, 1–20.

Trimaille, T., Pichot, C., Elaïssari, A., Fessi, H., Briancon, S., Delair, T., 2003. Poly(D,L-lactic acid) nanoparticle preparation and colloidal characterization. Colloid Polym. Sci. 281, 1184–1190.

Wakabayashi, A., Sasakawa, Y., Dobashi, T., Yamamoto, T., 2006. Self-assembly of tin oxide nanoparticles: localized percolating network formation in polymer matrix. Langmuir 22, 9260–9263.

Vijayaraj Kumar, P., Jain, N.K., 2007. Suppression of agglomeration of ciprofloxacin-loaded human serum albumin nanoparticles. AAPS PharmSciTech. 8, article 17.

Wolert, E., Setz, S.M., Underhill, R.S., Duran, R.S., Schappacher, M., Deffieux, A., Holderle, M., Mulhaupt, R., 2001. Meso- and microscopic behavior of spherical polymer particles assembling at the air–water interface. Langmuir 17, 5671–5677.

Zhang, K.-w., Tang, F.-q., Long, J., 1991. Film-forming ability of submicrometer silica particles. Langmuir 7, 1293–1295.